Understanding Atomic-Scale Features of Low Temperature-Relaxation Dynamics in Metallic Glasses

B. Wang,[†,‡] B. S. Shang,[§] X. Q. Gao,[∥] W. H. Wang,[†] H. Y. Bai,[†] M. X. Pan,*,[†,‡] and P. F. Guan*,[§]

[†]Institute of Physics, Chinese Academy of Sciences, Beijing 100190, China

[‡]School of Physical Sciences, University of Chinese Academy of Sciences, Beijing 100094, China

[§]Beijing Computational Science Research Center, Beijing 100094, China

[∥]Northwest Institute for Nonferrous Metal Research, Xian 710016, China

S *Supporting Information*

ABSTRACT: Being a key feature of a glassy state, low temperature relaxation has important implications on the mechanical behavior of glasses; however, the mechanism of low temperature relaxation is still an open issue, which has been debated for decades. By systematically investigating the influences of cooling rate and pressure on low temperature relaxation in the $Zr_{50}Cu_{50}$ metallic glasses, it is found that even though pressure does induce pronounced local structural change, the low temperature-relaxation behavior of the metallic glass is affected mainly by cooling rate, not by pressure. According to the atomic displacement and connection mode analysis, we further demonstrate that the low temperature relaxation is dominated by the dispersion degree of fast dynamic atoms rather than the most probable atomic nonaffine displacement. Our finding provides the direct atomic-level evidence that the intrinsic heterogeneity is the key factor that determines the low temperature-relaxation behavior of the metallic glasses.
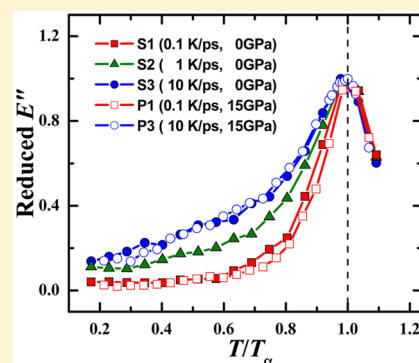
Glass is usually made by fast quenching of a high-temperature liquid, which is in a nonequilibrium metastable state.[1,2] As a result, the relaxation behavior of glass-forming systems diversifies;[3−5] that is, only one relaxation mode is present in the glass-forming liquid at a sufficient high temperature, while it seems to split into two modes, primary relaxation (so-called α relaxation) and secondary or Johari−Goldstein relaxation (so-called β-relaxation), when the temperature drops into the supercooled liquid regime.[3−9] At the glass-transition temperature (T_g), the α-relaxation is frozen while the β-relaxation still remains, even below T_g, which becomes the source of glass dynamics at low temperature, and it is important for us to understand many physical properties of glassy solids.[3,9,10] In the broad glass literature, the physical nature of low temperature relaxation has been debated for decades, which still constitutes one of the vital topics as of today.[9−22] Metallic glasses (MGs) are often being viewed as a simple glass system made up of atoms randomly distributed in a disordered structure, which constitutes an ideal system to study the low temperature-relaxation behavior.

Recently, some experimental results showed that the low temperature relaxation in MGs could be related to shear transformation zones (STZs)[22−24] and diffusion of atoms[25,26] and has significant influence on tensile plasticity[27] and fragility.[20] However, no consensus has been reached yet on whether low temperature relaxation is of a local or cooperative motion.[25,26] Some researchers believed that low temperature relaxation acts as a precursor of α-relaxation,[8,17,28] while others claimed that low temperature relaxation has an independent

relaxation mechanism.[29] Previous theoretical and experimental works suggested that low temperature relaxation (or internal friction) of MGs could be attributed to "fast" or "mobile" atoms[14] and strongly correlated with the spatial heterogeneity.[30] Recently, Yu et al.[31] claimed that the viscoelastic moduli for one glass state under different time scales are mainly determined by the most probable atomic nonaffine displacements rather than the fast-moving atoms. However, because glass is in a nonequilibrium state due to fast quenching, the state or atomic structure of metallic glass can be significantly tuned by changing the cooling rate[12] or pressure.[32,33] Thus it should be interesting to investigate the cooling rate and pressure dependence of low temperature-relaxation behaviors and thereby the atomic level mechanism of low temperature relaxation in metallic glasses.

In this work, MD simulations that combine dynamic mechanical spectroscopy (MD−DMS) method and isoconfigurational ensemble were employed to investigate the low temperature-relaxation behavior and motion of each atom in the $Zr_{50}Cu_{50}$ MGs with different cooling rates and pressures. It is found that the low temperature relaxation is affected by cooling rate but not by pressure, even though pressure does induce pronounced local structure changes. Unfortunately, the most probable atomic nonaffine displacement[31] is not a good

parameter to describe the cooling rate and pressure effects. According to the atomic displacement and connection mode analysis, we conclude that the dispersion degree of atoms with large displacement is correlated with the intensity of low temperature relaxation. This provides direct evidence from the atomic level that the intrinsic heterogeneity is the key factor in determining the low temperature-relaxation behavior of the metallic glass, which is supported by recent experimental results.[30]

The details of our model systems and MD−DMS method are presented in the Simulation Methods and Supporting Information (Figure S1). In brief, glassy samples are prepared by different cooling rates under various pressures. The features of these samples are listed in Table S1. All samples can be separated into two groups: zero-pressure samples with different cooling rates (denoted as S1, S2, and S3) for considering the cooling rate effect and the corresponding high-pressure samples (denoted as P1 and P3) for investigating the pressure effect. First, we present how the state of metallic glasses is tuned by the cooling rate and pressure during the quenching process. The difference between the total energy, E, and the energy of harmonic vibrations ($3k_BT$) as a function of temperature, T, for various systems is shown in Figure 1a. For each system, we can define the T_g as the crossover temperature between the behaviors of $E − 3k_BT$ for lower temperatures and higher temperatures. Obviously, the T_g is affected not only by cooling rate but also by pressure, which is consistent with the previous works.[12,32,33] This indicates that the atomic structure of these samples should be different. The total radial distribution functions (RDFs) of S1, S3, P1, and P3 are shown in Figure 1b. The pressure introduces more pronounced changes to the atomic structure than cooling rate from the RDF perspective. The left shift of the first peak indicates the higher density, and the weakness of first peak intensity suggests the averaged atomic number decreases in the first neighbor shell. The obvious splitting of the second peak implies the enhanced medium range order in high-pressure samples. For more information about the pressure effect, the partial RDFs and the averaged coordination numbers are shown in Figure S2. Obviously, all of these influences could be represented by the local atomic packing information. As shown in Figure 1c, pressure does induce pronounced local structure changes, such as the fraction of <0,0,12,0> cluster (denoted as f_{ico}). By comparing the data of S1 and P1, the f_{ico} increases nearly three times due to the high-pressure effect, which is comparable to the results in ref 33. Because both the cooling rate and pressure could affect the atomic configuration (state) of metallic glasses, the low temperature-relaxation behavior should represent the cooling rate effect and pressure effect. Furthermore, the pressure effect should be stronger according to the dramatic structure changes under higher pressure.

On the basis of the systematic MD−DMS simulations, the loss moduli E'' as a function of T for various samples are shown in Figure 2a. All of the E'' curves exhibit a peak at T_α corresponding to the α-relaxation, which signals the transition from glassy to supercooled liquid states. It is found that there is almost no influence on T_α for the samples with different cooling rates, which is consistent with previous results.[34] The right shift of T_α for higher pressure samples is consistent with the conclusion that the glass-transition temperature increases as pressure increases (see Figure 1a). According to the conclusion in ref 31, we may obtain the collapse of data E'' as a function of u_p, the most probable atomic nonaffine displacement. To
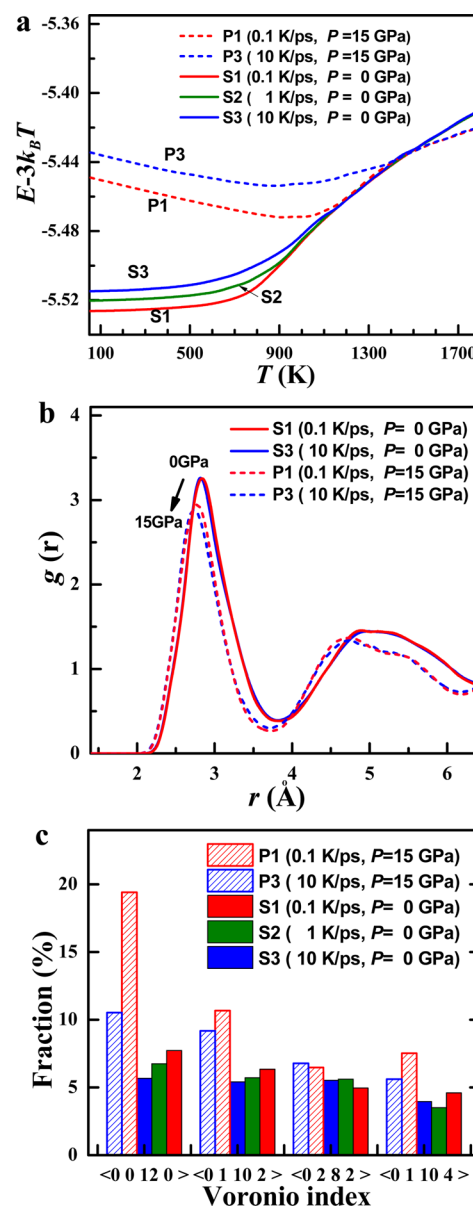

Figure 1. Fundamental structural information on all samples tested. (a) Difference between total energy and the energy of harmonic vibrations ($3k_BT$) as a function of temperature for samples with various cooling rates and different pressures. (b) Atomic pair correlation functions $g(r)$ of all atoms for samples of S1, S3, P1, and P3. (c) Histogram of Voronoi clusters for all of the samples (S1, S2, S3, P1, and P3). The simulated temperature is 300 K.

confirm this inference, we calculated $u_i(t_p)$, the mean square atomic displacement for each atom i within time interval t_p for all simulated samples, and obtained the probability distribution density function $p(u)$ (see the Supporting Information for more details). The $p(u)$ for different temperatures of each sample are shown in Figure S3, and the non-Gaussian distribution suggests the heterogeneous atomic level dynamics during the cycle loading. As shown in Figure 2b, we plotted E'' as a function of u_p, the peak position of $p(u)$ for all samples. Unfortunately, we do not obtain the collapse of data for these samples. This means that the scaling between E'' and u_p obtained based on the same materials but at different frequencies is not appropriate for describing the influence of cooling rate and pressure on low temperature relaxation.
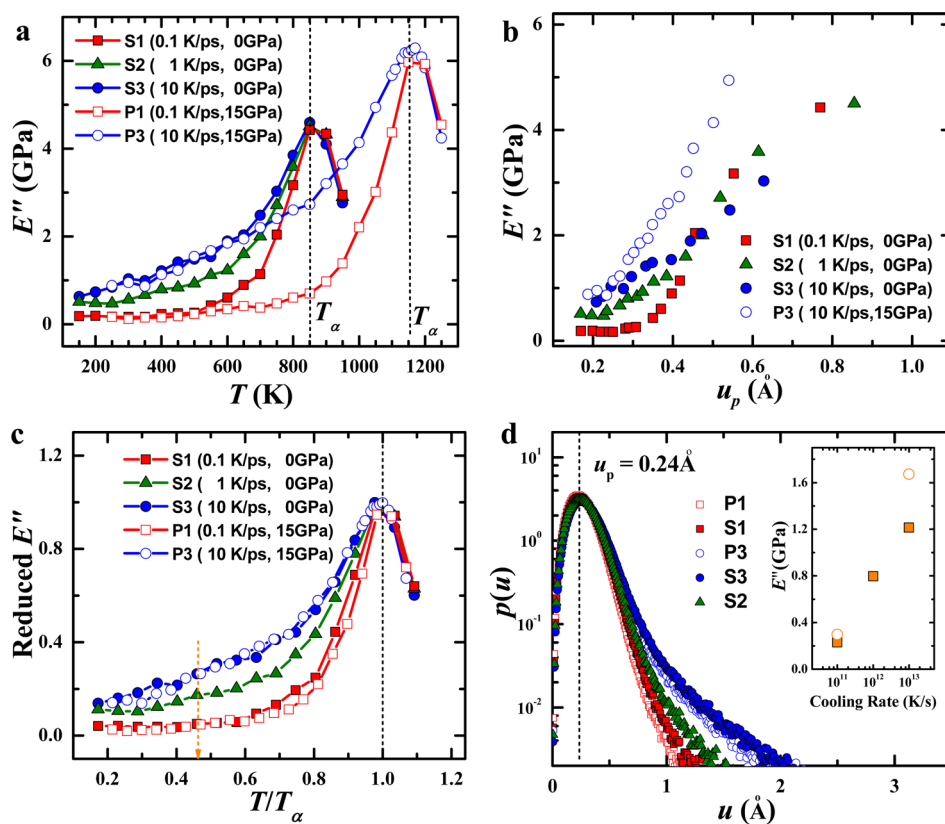
Figure 2. Loss modulus and the atomic displacement information. (a) Temperature dependence of loss modulus E'' for samples with various cooling rates and pressures. The filled symbols are results of the zero-pressure samples. The open ones present results of the high-pressure (15 GPa) samples. (b) E'' as a function of u_p. u_p represents the most probable atomic nonaffine displacement.(c) Reduced loss modulus E''/E''_{peak} as a function of T/T_α. (d) $p(u)$ for different samples at the scaled temperature $T/T_\alpha = 0.47$. The inset of panel d shows the E'' for different samples at $T/T_\alpha = 0.47$.

To understand the intrinsic behaviors of low temperature relaxation, we plotted the reduced loss modulus E''/E''_{peak} as a function of T/T_α for avoiding the effects of T_α and the peak intensity. The reduced loss modulus curves for various samples are shown in Figure 2c. In general, the value of E''/E''_{peak} decreases as cooling rate decreases at low scaled temperatures. This suggests that the relative intensity of low temperature relaxation reduces as the cooling rate decreases, which is consistent with the experimental works.[30,34,35] Furthermore, it is amazing to find the collapse of the E''/E''_{peak} curves for samples (S1 and P1, S3 and P3) with the same cooling rate, even though the pressure is different. The collapse indicates that the cooling rate dominates the essential properties of low temperature relaxation in MGs. This reveals that low temperature relaxation is affected by cooling rate, but not by pressure, even though pressure does induce pronounced local structure changes. So, it should be interesting to study whether there is an important parameter dominating the low temperature relaxation.

To find the hints for understanding the intrinsic parameter of low temperature relaxation, we analyzed the atomic-level dynamic properties of each sample. As shown in Figure 2d, we plotted $p(u)$ for each sample at the same reduced temperature $T/T_\alpha = 0.47$. We were surprised to find that these curves have the same value of $u_p = 0.24 \pm 0.02$ Å but appreciable difference at the tails of $p(u)$ when $u > 0.50$ Å. Remarkably, the related values of E'' are different for these samples (see inset of Figure 2d). This implies that the most probable atomic nonaffine displacement u_p for different samples

is mainly determined by the reduced temperature T/T_α, at least under the same loading frequency $1/t_p$. The collapse of $p(u)$ curves for samples with same value of E''/E''_{peak} suggests that the reduced loss modulus is determined by the tail of $p(u)$. Moreover, the fast dynamic atoms can be viewed as major contributors to the relaxation[14] and the microscopic features of fast atoms may help us to understand the features of low temperature-relaxation dynamics.

Here we selected the top 5% of atoms with the largest displacements (400 atoms, based on the $p(u)$ in Figure 2d for each sample to characterize the microscopic features of the fast dynamic atoms). However, there no strong correlation can be extracted between the low temperature-relaxation intensity and the microscopic features of these selected atoms, such as the free volume and potential energy, except for the spatial connection method of these atoms. To characterize the spatial connection behaviors, we calculated the possibility of forming clusters by these atoms.[36] The inset of Figure 3a presents the discrete counts of the clusters with different sizes for various samples. It exhibits a power-law distribution from the small to intermediate size clusters and the obvious deviation for large clusters[37,38] for samples with different cooling rates. The fractions of the clusters with larger sizes are shown in Figure 3a. It is clear to see that the samples with higher cooling rate tend to form larger clusters, which indicates the aggregation of fast atoms in faster quenched MG systems. However, pressure has almost no influence on the packing method of these atoms. To further investigate the spatial distribution of clusters, we analyzed the connectivity of these atoms. The connectivity
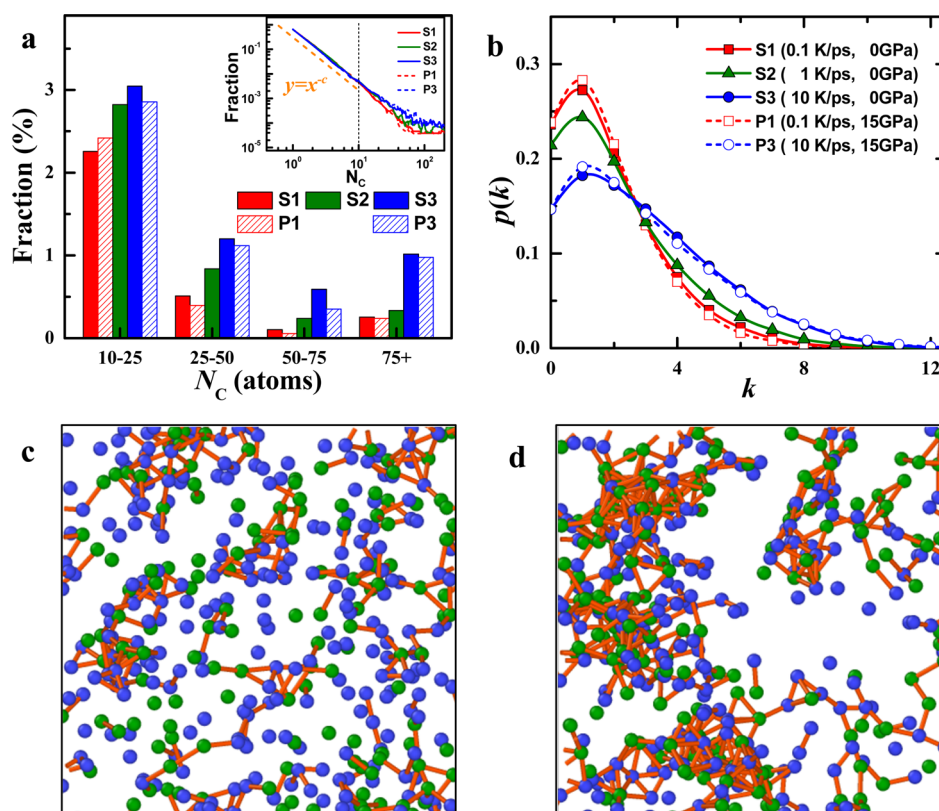
Figure 3. Connectivity and spatial heterogeneity of selected 5% atoms with largest displacements. (a) Histogram of the clusters with larger sizes (more than 10 atoms). The inset of panel a is the special distribution of the selected atoms. (b) Connectivity distribution of the selected atoms. (c,d) 2D snapshots of atomic connectivity in S1 and S3 at the scaled temperature $T/T_{\alpha} = 0.47$, respectively. The green atoms represent zirconium and the blue atoms represent copper. The orange lines exhibit the atomic bonding with a cutoff distance $d_c = 3.8$ Å.

degree k of atom i is defined as the number of selected atoms in its nearest-neighbor shell. The distribution of connectivity degree k is characterized by $p(k)$, which gives the probability that an atom is connected to k selected atoms.[36] The higher $p(k)$ at large k presents a higher probability for forming big clusters, which reflects a lower dispersion degree of atoms. As shown in Figure 3b, the broadening distribution of $p(k)$ for the faster quenched samples confirms that the dispersion degree of these atoms increases as the cooling rate decreases but depends less on pressure, which is consistent with the results of E''/E''_{peak}. The spatial distribution and connection behaviors of these atoms at scaled temperature of 0.47 are shown in Figure 3c,d for S1 and S3, respectively. The more evident spatial heterogeneity of these atoms in faster quenched sample S3 with stronger low temperature relaxation indicates the correlation between the low temperature relaxation and the spatial heterogeneity in MGs, which is consistent with the recent experimental results.[30] The weak influence of pressure to $p(k)$ suggests that the spatial heterogeneity of fast dynamic atoms in MG is mainly controlled by cooling rate rather than pressure in our studied pressure range. The outcome provides the direct evidence from atomic level that the intrinsic heterogeneity is the key parameter that determines the low temperature-relaxation behavior of the metallic glass. The reason why the dynamical spatial heterogeneity is mainly controlled by cooling rate but not pressure and the relation between intrinsic dynamical heterogeneity and local structure will be discussed in the future work. On contrary, the dynamic heterogeneity is a time-scale dependence parameter that is strongly correlated to the observation time. So, it is reasonable to observe different

dynamic heterogeneity behaviors for the same value of E'' under various loading frequencies in ref 14, and we may only compare the dynamic heterogeneity behaviors for DMS measurement on the same time scale or under the same loading frequency. Furthermore, it should be interesting to check whether u_p is correlated with T/T_{α} and the connection method (spatial heterogeneity) of fast atoms under different loading frequencies.

In summary, we have shown that the low temperature relaxation in metallic glass is mainly affected by cooling rate rather than by pressure. The spatial heterogeneity of atoms with fast mobility is responsible for low temperature-relaxation behaviors, which can be dramatically tuned by cooling rate rather than pressure. Our finding provides the direct atomic-level evidence that the intrinsic heterogeneity is the key factor that determines the low temperature-relaxation behavior and may shed light on how to understand the origin of relaxation in glassy materials.

■ SIMULATION METHODS

Molecular dynamics simulations have been performed by utilizing the open source code-LAMMPS.[39] The prototypical binary system $Zr_{50}Cu_{50}$ was selected for its superior glass-forming ability and the detail about the optimized embedded atom method (EAM) potential generated by Sheng et al. can be inferred from ref 40. Initially, 8000 atoms of the required composition are placed in a cubic box randomly, with periodic boundary conditions applied in all three directions. After equilibrating at 1900 K under various external hydrostatic pressures P (P = 0, 15.0 GPa) with the constant number,

pressure, and temperature (NPT) ensemble for at least 10 ns, samples are quenched to 50 K step by step at the various rates (0.1, 1.0, and 10 K/ps) with the NPT ensemble. For all simulations, the time step of integrating the equation of motion is 2 fs and the temperature is maintained by the Nosé−Hoover thermostat.

MD−DMS simulations that combine with isoconfigurational ensemble were employed for investigating the relaxation behavior in the $Zr_{50}Cu_{50}$ system. We apply a sinusoidal shear strain $\varepsilon(t) = \varepsilon_A \sin(2\pi t/t_p)$ along the xy direction of the model MG, where t_p represents the period of stress and ε_A means maximum strain value. Here t_p is selected as 100 ps and ε_A as 2% (which is in the linear elastic region) for all MD−DMS simulations. All of these MD−DMS measures were carried out in constant number, volume, and temperature (NVT) ensemble. To unravel the influence of the initial state on the resultant stress in the cyclic loading process, isoconfigurational ensemble introduced by Harrowell et al.[41,42] was employed: 50 independent sinusoidal shear deformation simulations were performed, which all started from the same initial configuration but with momenta randomly assigned from the Maxwell−Boltzmann distribution at the interested temperatures. For each MD−DMS loading, 10 full cycles were used; that is, t in the range $[0, 10\, t_p]$ and the mean stresses were fitted to the function $\sigma(t) = \sigma_0 + \sigma_A \sin(2\pi t/t_p + \delta)$, where σ_A is the maximum resultant stress and δ is the phase shift between the strain and the stress. Then, the storage (E') and the loss (E'') modulus were calculated with the formulas $E' = \sigma_A/\varepsilon_A \cos(\delta)$ and $E'' = \sigma_A/\varepsilon_A (\delta)$ (see the Supporting Information), respectively.

■ ASSOCIATED CONTENT

ⓢ Supporting Information

The Supporting Information is available free of charge on the ACS Publications website at DOI: 10.1021/acs.jpclett.6b02466.

Features and structures of samples used and intermediate processes of data analysis. (PDF)

■ AUTHOR INFORMATION

Corresponding Authors
*M.X.P.: E-mail: panmx@aphy.iphy.ac.cn.
*P.F.G.: E-mail: pguan@csrc.ac.cn.
ORCID ⓞ
P. F. Guan: 0000-0002-7679-6768
Notes
The authors declare no competing financial interest.

■ ACKNOWLEDGMENTS

■ REFERENCES

(1) Angell, C. A. The glass transition. Curr. Opin. *Curr. Opin. Solid State Mater. Sci.* **1996**, *1*, 578−585.

(2) Greer, A. L. Metallic glasses. *Science* **1995**, *267*, 1947−1953.

(3) Ngai, K. *Relaxation and Diffusion in Complex Systems*; Springer Science & Business Media: 2011.

(4) Dyre, J. Colloquium: The glass transition and elastic models of glass-forming liquids. *Rev. Mod. Phys.* **2006**, *78*, 953−972.

(5) Ediger, M. D.; Harrowell, P. Perspective: Supercooled liquids and glasses. *J. Chem. Phys.* **2012**, *137*, 080901.

(6) Hu, L.; Yue, Y. Secondary Relaxation in Metallic Glass Formers: Its Correlation with the Genuine Johari-Goldstein Relaxation. *J. Phys. Chem. C* **2009**, *113*, 15001−15006.

(7) Johari, G. P. Viscous Liquids and the Glass Transition. II. Secondary Relaxations in Glasses of Rigid Molecules. Jour. *J. Chem. Phys.* **1970**, *53*, 2372−2388.

(8) Ngai, K. L.; Paluch, M. Classification of secondary relaxation in glass-formers based on dynamic properties. *J. Chem. Phys.* **2004**, *120*, 857−873.

(9) Ngai, K. Correlation between the secondary β-relaxation time at T g with the Kohlrausch exponent of the primary α relaxation or the fragility of glass-forming materials. *Phys. Rev. E: Stat. Phys., Plasmas, Fluids, Relat. Interdiscip. Top.* **1998**, *57*, 7346−7349.

(10) Lu, Z.; Jiao, W.; Wang, W. H.; Bai, H. Y. Flow unit perspective on room temperature homogeneous plastic deformation in metallic glasses. *Phys. Rev. Lett.* **2014**, *113*, 045501.

(11) Goldstein, M. The past, present, and future of the Johari−Goldstein relaxation. *J. Non-Cryst. Solids* **2011**, *357*, 249−250.

(12) Wang, W. H.; Dong, C.; Shek, C. H. Bulk metallic glasses. *Mater. Sci. Eng., R* **2004**, *44*, 45−89.

(13) Ashby, M.; Greer, A. Metallic glasses as structural materials. *Scr. Mater.* **2006**, *54*, 321−326.

(14) Yu, H.-B.; Samwer, K. Atomic mechanism of internal friction in a model metallic glass. *Phys. Rev. B: Condens. Matter Mater. Phys.* **2014**, *90*, 144201.

(15) Angell, C. A.; Ngai, K. L.; McKenna, G. B.; McMillan, P. F.; Martin, S. W. Relaxation in glassforming liquids and amorphous solids. *J. Appl. Phys.* **2000**, *88*, 3113−3157.

(16) Cohen, Y.; Karmakar, S.; Procaccia, I.; Samwer, K. The nature of the β-peak in the loss modulus of amorphous solids. *EuroPhys. Lett.* **2012**, *100*, 36003.

(17) Dixon, P. K.; Wu, L.; Nagel, S. R.; Williams, B. D.; Carini, J. P. Scaling in the relaxation of supercooled liquids. *Phys. Rev. Lett.* **1990**, *65*, 1108−1111.

(18) Fan, Y.; Iwashita, T.; Egami, T. Crossover from Localized to Cascade Relaxations in Metallic Glasses. *Phys. Rev. Lett.* **2015**, *115*, 045501.

(19) Hachenberg, J. r.; Bedorf, D.; Samwer, K.; Richert, R.; Kahl, A.; Demetriou, M. D.; Johnson, W. L. Merging of the α and β relaxations and aging via the Johari−Goldstein modes in rapidly quenched metallic glasses. *Appl. Phys. Lett.* **2008**, *92*, 131911.

(20) Yu, H. B.; Wang, Z.; Wang, W. H.; Bai, H. Y. Relation between β relaxation and fragility in LaCe-based metallic glasses. *J. Non-Cryst. Solids* **2012**, *358*, 869−871.

(21) Yu, H. B.; Samwer, K.; Wang, W. H.; Bai, H. Y. Chemical influence on b-relaxations and the formation of molecule-like metallic glasses. *Nat. Commun.* **2013**, *4*, 2204.

(22) Yu, H. B.; Wang, W. H.; Bai, H. Y.; Wu, Y.; Chen, M. W. Relating activation of shear transformation zones to β relaxations in metallic glasses. *Phys. Rev. B: Condens. Matter Mater. Phys.* **2010**, *81*, 220201.

(23) Yu, H. B.; Wang, W. H.; Samwer, K. The beta relaxation in metallic glasses: an overview. *Mater. Today* **2013**, *16*, 183−191.

(24) Yu, H. B.; Wang, W. H.; Bai, H. Y.; Samwer, K. The β-relaxation in metallic glasses. *Nat. Sci. Rev.* **2014**, *1*, 429−461.

(25) Yu, H. B.; Samwer, K.; Wu, Y.; Wang, W. H. Correlation between β Relaxation and Self-Diffusion of the Smallest Constituting Atoms in Metallic Glasses. *Phys. Rev. Lett.* **2012**, *109*, 095508.

(26) Liu, Y. H.; Fujita, T.; Aji, D. P.; Matsuura, M.; Chen, M. W. Structural origins of Johari-Goldstein relaxation in a metallic glass. *Nat. Commun.* **2014**, *5*, 3238.

(27) Yu, H. B.; Shen, X.; Wang, Z.; Gu, L.; Wang, W. H.; Bai, H. Y. Tensile Plasticity in Metallic Glasses with Pronounced β Relaxations. *Phys. Rev. Lett.* **2012**, *108*, 015504.

(28) Harmon, J. S.; Demetriou, M. D.; Johnson, W. L.; Samwer, K. Anelastic to plastic transition in metallic glass-forming liquids. *Phys. Rev. Lett.* **2007**, *99*, 135502.

(29) Schneider, U.; Brand, R.; Lunkenheimer, P.; Loidl, A. Excess wing in the dielectric loss of glass formers: A Johari-Goldstein β relaxation? Phys. *Phys. Rev. Lett.* **2000**, *84*, 5560−5563.

(30) Zhu, F.; Nguyen, H. K.; Song, S. X.; Aji, D. P.; Hirata, A.; Wang, H.; Nakajima, K.; Chen, M. W. Intrinsic correlation between beta-relaxation and spatial heterogeneity in a metallic glass. *Nat. Commun.* **2016**, *7*, 11516.

(31) Yu, H. B.; Richert, R.; Samwer, K. Correlation between Viscoelastic Moduli and Atomic Rearrangements in Metallic Glasses. *J. Phys. Chem. Lett.* **2016**, *7*, 3747−3751.

(32) Lou, H. B.; Xiong, L. H.; Ahmad, A. S.; Li, A. G.; Yang, K.; Glazyrin, K.; Liermann, H. P.; Franz, H.; Wang, X. D.; Cao, Q. P.; Zhang, D. X.; Jiang, J. Z. Atomic structure of Pd81Si19 glassy alloy under high pressure. *Acta Mater.* **2014**, *81*, 420−427.

(33) Ding, J.; Asta, M.; Ritchie, R. O. Anomalous structure-property relationships in metallic glasses through pressure-mediated glass formation. *Phys. Rev. B: Condens. Matter Mater. Phys.* **2016**, *93*, 140204.

(34) Zhao, L. Z.; Wang, W. H.; Bai, H. Y. Modulation of β-relaxation by modifying structural configurations in metallic glasses. *J. Non-Cryst. Solids* **2014**, *405*, 207−210.

(35) Yu, H. B.; Tylinski, M.; Guiseppi-Elie, A.; Ediger, M. D.; Richert, R. Suppression of beta Relaxation in Vapor-Deposited Ultrastable Glasses. *Phys. Rev. Lett.* **2015**, *115*, 185501.

(36) Shang, B. S.; Li, M. Z.; Yao, Y. G.; Lu, Y. J.; Wang, W. H. Evolution of atomic rearrangements in deformation in metallic glasses. *Phys. Rev. E* **2014**, *90*, 042303.

(37) Sethna, J. P.; Dahmen, K. A.; Myers, C. R. Crackling noise. *Nature* **2001**, *410*, 242−250.

(38) Krisponeit, J. O.; Pitikaris, S.; Avila, K. E.; Kuchemann, S.; Kruger, A.; Samwer, K. Crossover from random three-dimensional avalanches to correlated nano shear bands in metallic glasses. *Nat. Commun.* **2014**, *5*, 3616.

(39) Plimpton, S. Fast parallel algorithms for short-range molecular dynamics. *J. Comput. Phys.* **1995**, *117*, 1−19.

(40) Cheng, Y. Q.; Sheng, H. W.; Ma, E. Relationship between structure, dynamics, and mechanical properties in metallic glass-forming alloys. *Phys. Rev. B: Condens. Matter Mater. Phys.* **2008**, *78*, 014207.

(41) Widmer-Cooper, A.; Harrowell, P.; Fynewever, H. How reproducible are dynamic heterogeneities in a supercooled liquid? Phys. *Phys. Rev. Lett.* **2004**, *93*, 135701.

(42) Widmer-Cooper, A.; Harrowell, P. Predicting the long-time dynamic heterogeneity in a supercooled liquid on the basis of short-time heterogeneities. *Phys. Rev. Lett.* **2006**, *96*, 185701.